High-pressure Raman scattering study on zircon- to scheelite-type structural phase transitions of RCrO$_4$

Y. W. Long, L. X. Yang, Y. Yu, F. Y. Li, Y. X. Lu, R. C. Yu, Y. L. Liu, and C. Q. Jin[a)]
National Laboratory for Condensed Matter Physics, Institute of Physics, Chinese Academy of Sciences, Beijing 100080, People's Republic of China

(Received 8 November 2007; accepted 22 February 2008; published online 14 May 2008)

High-pressure Raman scattering experiments were performed on the zircon-type RCrO$_4$ (R=Nd, Dy) compounds with the space group $I4_1/amd$ by using diamond anvil cell techniques at room temperature. These two compounds exhibit similar Raman behaviors. Pressure-induced structural phase transitions were observed at the onset of 1.3 and 4.1 GPa for R=Nd and Dy, respectively. Moreover, pressure-released Raman spectra indicate that the structural transitions are irreversible. The high-pressure new phases were convincingly confirmed to be the scheelite structure in $I4_1/a$ symmetry based on the same Raman vibrations between the pressure-released DyCrO$_4$ and the scheelite-type DyCrO$_4$ synthesized at 6 GPa and 450 °C. In addition, we also calculated the bulk moduli according to Errandonea's method as well as the mode Grüneisen parameters of RCrO$_4$.
 [DOI: 10.1063/1.2909202]

I. INTRODUCTION

The zircon-type structure with the chemical composition of ABX_4 is named after the important mineral zircon ZrSiO$_4$, which crystallizes into a tetragonal lattice with the space group $I4_1/amd$ (D_{4h}^{19}, No. 141, Z=4) at ambient conditions. The crystal structure of zircon is characterized by AX_8 dodecahedrons with eight close A-X distances and isolated and slightly distorted BX_4 tetrahedrons.[1] Zircon-type compounds are fairly common in nature and can form into lots of charge combinations at A and B sites. For example, the compounds $Ca^{2+}Cr^{6+}O_4$,[2] $Y^{3+}V^{5+}O_4$,[3] $Hf^{4+}Si^{4+}O_4$,[4] and $Ta^{5+}B^{3+}O_4$ (Ref. 5) with different charge couplings crystallize into the zircon-type structure at normal conditions. Therefore, zircon-type materials extensively exhibit physical and chemical properties.

Most of the results obtained from experiments and theoretical calculations have shown that the zircon-type structure is rather sensitive to external pressure and temperature. For instance, a lower symmetry phase (orthorhombic) was observed in the zircon-type TbMO$_4$ and DyMO$_4$ (M=Cr, V) compounds at low temperature.[6–9] In particular, the tetragonal zircon-type phase usually transforms into another tetragonal scheelite-type structure accompanying the reduction of symmetry into $I4_1/a$ (C_{4h}^6, No. 88, Z=4) under a high pressure.[10–19] It is well known that material properties are closely related to the correlated structure. Therefore, it is interesting to study the pressure-related structures and properties of zircon-type compounds.

The family of RECrO$_4$ have the zircon-type crystal structure at ambient conditions, where RE stands for rare earth elements except for La and Ce. They were primarily prepared by using the solid-state reaction method several decades ago.[20] However, a small quantity of impurities such as Cr_2O_3 always occurred when using this method. In the past several years, a series of single phase zircon-type RECrO$_4$ compounds were obtained owing to the advancement in synthesis methods.[9,21–23] Furthermore, their magnetic properties have also been extensively investigated, taking into account the unusual valence state of chromium (V) ions in RECrO$_4$.[9,21–27] We recently observed a pressure-induced irreversible structural phase transition from the zircon to the scheelite structure in YCrO$_4$.[28] Moreover, a ferromagnetic to antiferromagnetic transition was also observed accompanying the structural phase transition.[29]

In the present paper, we report a high-pressure structural study on the zircon-type RCrO$_4$ (R=Nd, Dy) by using Raman scattering methods at room temperature. Pressure-driven, zircon-scheelite irreversible structural phase transitions were observed in them, and the mode Grüneisen parameters were calculated.

II. EXPERIMENTAL

According to the synthesis procedure proposed by Saez-Puche *et al.*,[22] zircon-type RCrO$_4$ polycrystalline samples were prepared by using highly pure (>99.9%) $R(NO_3)_3\cdot 6H_2O$ and $Cr(NO_3)_3\cdot 9H_2O$ as starting materials. The stoichiometric nitrates were fully mixed and ground in a mortar. Then, a special thermal treatment was performed on the mixture in oxygen flow as follows: 2 °C/min to 160 °C for 30 min, 2 °C/min to 200 °C for 30 min, and then 10 °C/min to 580 °C for 60 min. Finally, green color zircon-type RCrO$_4$ compounds were obtained with natural furnace cooling.

Pressure was generated by using a Mao–Bell-type diamond anvil cell (DAC) with 0.5 mm diamond culets. T301 stainless steel preindented up to 10 GPa with a thickness of 0.05 mm was used as the gasket, where a small hole of 0.2 mm in diameter was drilled as the sample chamber. RCrO$_4$ polycrystalline powder and a few of ruby grains used as

[a)]Author to whom correspondence should be addressed. Electronic mail: jin@aphy.iphy.ac.cn.

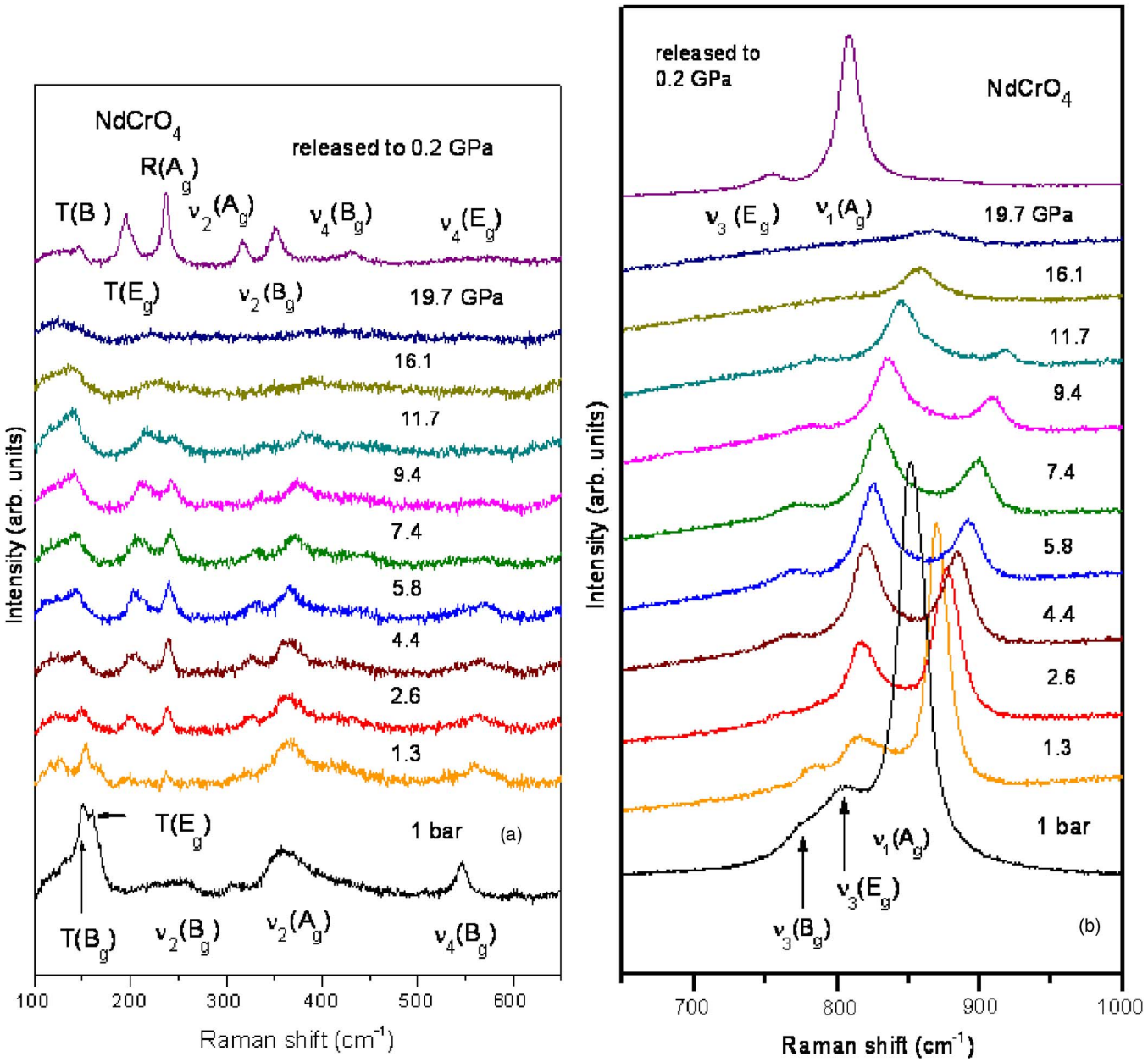

FIG. 1. (Color online) Pressure-related Raman spectra of $NdCrO_4$ at (a) the lower and (b) the higher frequency regions.

pressure calibrant were carefully loaded into the chamber. In order to obtain a hydrostatic pressure condition, a mixture of methanol and ethanol with a molar ratio of 4:1 was applied as the pressure transmitting medium. The pressure was measured by using the ruby fluorescence method.[30]

Raman spectroscopic measurements were performed by using a LABRAM–HR confocal laser micro-Raman spectrometer (HR800) equipped with a charge-couple device detector in backscattering geometry. Raman spectra at different pressures were collected in the frequency range from 100 to 1000 cm^{-1} with a 1 cm^{-1} resolution. For Raman excitation, the 532 nm line from a Verdi-2 solid-state laser was used. Due to the thermal instability of $RCrO_4$, the laser power was set to a lower level ($\sim$1 mW). The recording time was 100 s for each Raman spectrum. In order to focus the laser beam and collect the scattered light, a 25× microscope objective lens was adopted. All of the measurements reported here were carried out at room temperature.

III. RESULTS AND DISCUSSION

A. Ambient-pressure Raman spectra

Figures 1 and 2 show a series of Raman spectra of $RCrO_4$ at various pressures. The bottom patterns represent the ambient-pressure Raman spectra. Both $NdCrO_4$ and $DyCrO_4$ exhibit similar Raman behaviors since they have the same zircon-type crystal structure. A group theory analysis indicated that there exist 12 Raman active modes ($2A_{1g}+4B_{1g}+B_{2g}+5E_g$) for the zircon-type structure with the space group $I4_1/amd$ (D_{4h}^{19}).[31] Eight of them are observed in our experiments on the polycrystalline samples. It is possible that some polarized phonon modes are overlapped in the samples.[32] In addition, some weak Raman modes probably cannot be discerned in our experiment. All of these are responsible for the partial "missing" of Raman modes in the present paper.

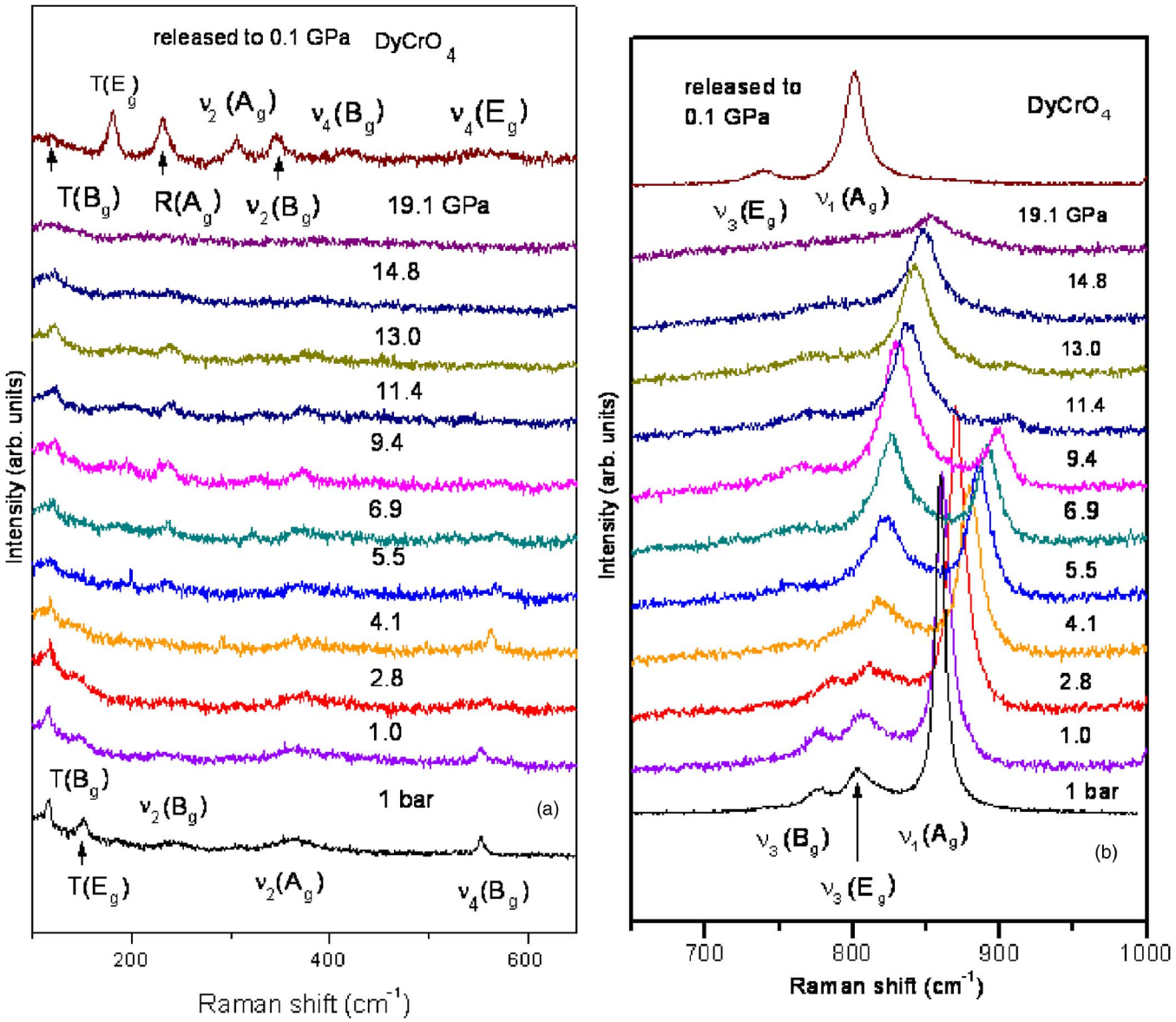

FIG. 2. (Color online) Pressure-related Raman spectra of $DyCrO_4$ at (a) the lower and (b) the higher frequency regions.

The Raman active modes of the zircon-type $RCrO_4$ were assigned based on the method proposed by Jayaraman *et al.*[10,11] to the isostructural $LnVO_4$ (Ln=Y, Tb, Dy) compounds, as shown in Figs. 1 and 2. Specifically, six Raman peaks were assigned as the internal vibration modes of CrO_4 tetrahedrons: stretching ν_1 (A_g) and ν_3 (B_g and E_g) modes and bending ν_2 (A_g and B_g) and ν_4 (B_g) modes; the other two were assigned as the external translation modes of CrO_4 polyhedrons: T (B_g and E_g). Because the Raman intensity of the stretching modes, which reflects the vibrations of Cr–O bonds in CrO_4 units, is much stronger than those of other modes, the Raman spectra were separately shown in two different phonon frequency regions in this paper: (a) 100–650 cm^{-1} and (b) 650–1000 cm^{-1}.

It has been reported that as a general rule in the zircon-type compounds, the ν_1 and ν_3 modes appear in a higher frequency region than other modes, and the intensity of the ν_1 mode is the strongest and the ν_2 mode is the weakest.[33] The Raman vibrational behaviors of $RCrO_4$ are well accordant with this rule at ambient conditions. When we compare the Raman spectra of $NdCrO_4$ and $DyCrO_4$, the ν_3 (B_g and E_g) modes tend to overlap in $NdCrO_4$, while they are obviously separated in $DyCrO_4$. In addition, the phonon frequency of the ν_1 mode is somewhat larger in $DyCrO_4$ (860 cm^{-1}) than that in $NdCrO_4$ (852 cm^{-1}). These results are related to the different bond lengths and angles of CrO_4 tetrahedrons in them.[9]

B. Pressure-related Raman spectra

In the beginning, we will describe the pressure-related Raman spectra of $NdCrO_4$. When the pressure increases to 1.3 GPa, abrupt changes in Raman spectrum take place compared to that at normal pressure, as presented in Figs. 1(a) and 1(b). In the lower frequency region (100–650 cm^{-1}), a series of new Raman peaks appear at 153, 196, 238, 324, 364, and 559 cm^{-1}, respectively. The most distinct change is the occurrence of the new Raman peaks at 196 and

238 cm^{-1}. These features are indicative of a pressure-induced structural phase transition. As we will describe later, the new high-pressure phase is identified to be a tetragonal scheelite-type structure with the space group $I4_1/a$. By a comparison of the phonon frequency, Raman intensity, and pressure coefficient of the new Raman peaks to those of other scheelite-type compounds reported by Manjon *et al.*,[34] the new Raman modes that appeared in $NdCrO_4$ are assigned as shown in Fig. 1. It should be noted that it is difficult to accurately record the phonon frequency of the new-phase ν_4 (B_g) mode due to its broadening under pressure.

In the higher frequency region (650–1000 cm^{-1}), the zircon-phase ν_3 (B_g and E_g) modes of $NdCrO_4$ have been thoroughly separated at 1.3 GPa, and the intensity of ν_1 (A_g) mode becomes much lower. Interestingly, the relative intensity of the ν_3 (E_g) versus the ν_1 (A_g) modes noticeably increases, as presented in Fig. 2(b). This feature implies the presence of a structural phase transition. A reasonable explanation is that a new Raman peak occurs at a similar frequency as that of the zircon-type ν_3 (E_g) mode at 1.3 GPa. Moreover, this new Raman peak can be assigned as the strongest Raman mode ν_1 (A_g) of the scheelite-type new phase. With increasing pressure, the ν_1 (A_g) mode of the new phase gradually strengthens, and the reverse is true for the zircon-type ν_1 (A_g) mode, which completely disappears at 16.1 GPa. In addition, the zircon-phase ν_3 (B_g) mode becomes ambiguous as the pressure increases to 2.6 GPa, at which another new Raman mode ν_3 (E_g) starts to emerge and becomes clear with the pressure up to 4.4 GPa.

As shown in Fig. 1, the total Raman intensity quickly lowers when the pressure exceeds 11.7 GPa. Moreover, the pressure-driven structural transition is sluggish at room temperature. Within the pressure range from 1.3 to 11.7 GPa, the zircon phase and the scheelite-type new phase always coexist. When the pressure reaches the highest value of 19.7 GPa that was used in this experiment, it is difficult to identify the Raman modes due to the peak broadening effect. Finally, the pressure is slowly released to 0.2 GPa, and only the Raman modes of the scheelite phase are observed. It means that the structural phase transition occurred in $NdCrO_4$ at the onset of 1.3 GPa is irreversible.

For $DyCrO_4$, the pressure-related Raman spectra are shown in Figs. 2(a) and 2(b). In the lower frequency region, the Raman vibrational intensity is somewhat weaker than that of $NdCrO_4$. However, the characteristic features of structural transition are unambiguous. When the pressure gradually increases to 4.1 GPa, new Raman peaks are clearly observed at the lower frequency region. In addition, the zircon-phase ν_3 (B_g) mode becomes indiscernible at this pressure. Just like the case observed in $NdCrO_4$, the relative intensity of the ν_3 (E_g) versus the ν_1 (A_g) modes also strongly increases in $DyCrO_4$ at 4.1 GPa. These features indicate the appearance of the structural phase transition of $DyCrO_4$. With increasing pressure up to 9.4 GPa, the Raman peaks of the new phase become stronger and stronger. All the new Raman peaks observed in $DyCrO_4$ are also assigned based on the scheelite-type structure, as shown in Fig. 2.

When the pressure increases to 13.0 GPa, the zircon-phase ν_1 (A_g) mode of $DyCrO_4$ becomes very weak, and the Raman intensity of the new phase also decreases obviously. With the pressure up to 19.1 GPa, only the new-phase ν_1 (A_g) mode is discriminable. Similarly, the structural transition of $DyCrO_4$ is sluggish too. The zircon phase and the scheelite phase coexist between 4.1 and 13.0 GPa. The pressure-released Raman spectrum to 0.1 GPa shows that the high-pressure phase appeared in $DyCrO_4$ at 4.1 GPa is also quenchable at ambient conditions.

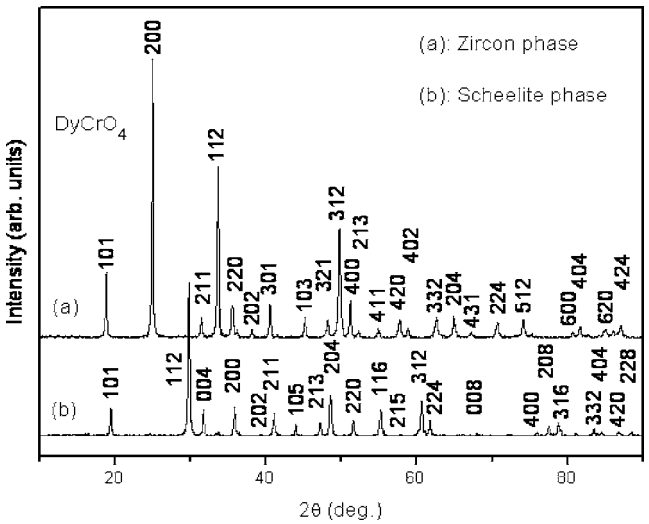

FIG. 3. Powder XRD patterns and the corresponding indices for (a) the zircon-type and (b) the scheelite-type $DyCrO_4$.

The broadening of Raman peaks at higher pressures can usually be ascribed to the reduction of the hydrostatic pressure environment in DAC, as well as pressure-induced structural disorder or even amorphization. Errandonea *et al.* gave a detailed description on the influence of pressure environment on structural transition.[35] In our previous study on the isostructural compound $CaCrO_4$, Raman peaks severely broadened with pressure up to 20 GPa.[18] However, fine x-ray diffraction (XRD) peaks were observed even if the pressure reached 30 GPa.[19] Therefore, the broadening of Raman peaks observed in $RCrO_4$ is most probably attributed to the reduction of the hydrostatic environment.

C. Determination of the new phases

$NdCrO_4$ and $DyCrO_4$ have the same zircon-type crystal structure at ambient pressure. Moreover, the new phases that appeared in both of them also exhibit similar Raman behaviors, as clearly shown by the pressure-released Raman spectra in Figs. 1 and 2. It means that they should have the same high-pressure phase.

The high-pressure structural properties of zircon-type compounds have been widely investigated experimentally. For example, high-pressure Raman scattering experiments were performed on $LnVO_4$,[10,11] and zircon-scheelite transitions were determined in them based on an XRD analysis of pressure-released samples. This kind of transition was subsequently confirmed by an *in situ* high-pressure synchrotron XRD experiment in YVO_4.[12] Most recently, we also observed the zircon-scheelite structural transition in $YCrO_4$ by using high-pressure Raman scattering and XRD methods.[28] $RCrO_4$ have the same ambient-pressure crystal structure as

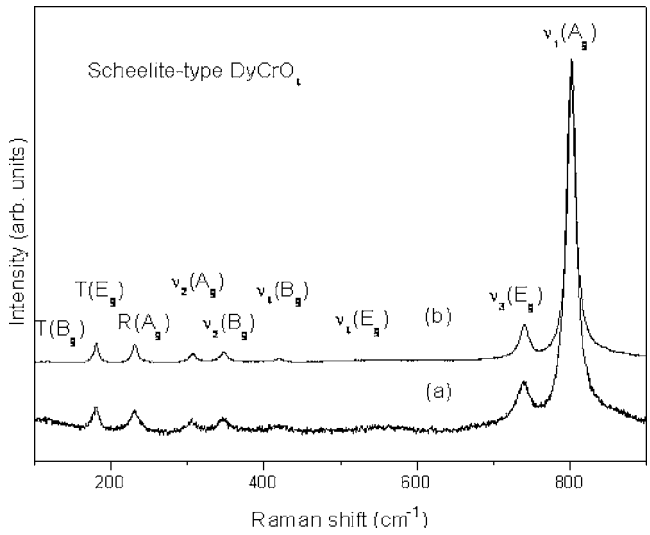

FIG. 4. Raman spectra of (a) the pressure-released $DyCrO_4$ to 0.1 GPa and (b) the scheelite-type $YCrO_4$ prepared at 6 GPa and 450 °C.

well as charge combination ($A^{3+}B^{5+}O_4$ type) with $LnVO_4$ and $YCrO_4$. Furthermore, the Raman behaviors of the high-pressure phases observed in $RCrO_4$ are very alike with those of the scheelite phase observed in $LnVO_4$ and $YCrO_4$. Therefore, we can infer that the new phases occurred in $RCrO_4$ also have the tetragonal scheelite-type structure with the space group $I4_1/a$ (C_{4h}^6). As a matter of fact, the zircon-scheelite structural conversion seems to be a universal phase transition route for zircon-type compounds under a moderate pressure and/or temperature.[36]

Due to the irreversibility of the structural transitions as well as the lower transition pressures of $RCrO_4$, a bulk scheelite-type $DyCrO_4$ was obtained at 6 GPa and 450 °C by using a cubic anvil high-pressure apparatus. Figure 3 shows the powder XRD patterns for the zircon-type $DyCrO_4$ as well as the quenched scheelite-type one. All the diffraction peaks can be indexed based on the correlated structural modes. A Rietveld structural analysis was performed. Table I shows the refined structural parameters such as lattice constants and atomic positions.

TABLE I. Crystallographic data for the zircon- and scheelite-type $DyCrO_4$. For the zircon phase, Dy and Cr atoms occupy the special sites 4*a* (0, 3/4, 1/8) and 4*b* (0, 1/4, 3/8), respectively. For the scheelite phase, Dy and Cr atoms occupy the special sites 4*b* (0, 1/4, 5/8) and 4*a* (0, 1/4, 1/8), respectively.

Formula	Zircon	Scheelite
Space group	$I4_1/amd$	$I4_1/a$
a (Å)	7.1364(2)	5.0157(1)
c (Å)	6.2687(2)	11.3196(3)
V (Å^3)	319.26(2)	284.52(2)
Z	4	4
O_x	0	0.2611(9)
O_y	0.4315(6)	0.1124(8)
O_z	0.2020(6)	0.0488(4)
R_{wp} (%)	11.40	8.32
R_p (%)	8.60	6.58

Raman scattering is one of the powerful tools to characterize material structure. In order to accurately identify the crystal structure of the new phases observed in $RCrO_4$, Raman scattering was also performed on the synthesized scheelite $DyCrO_4$ at ambient conditions. As obviously shown in Fig. 4, this scheelite-type compound exhibits the same Raman vibrations as those of the pressure-released $DyCrO_4$. Based on this fact, the new phases appeared in $RCrO_4$ in our high-pressure Raman experiments are convincingly assigned to the tetragonal scheelite-type structure, agreeing with well the compared results described above. Pressure-induced zircon-to-scheelite phase transition mechanism was discussed in detail in our recent report.[29]

D. Mode Grüneisen parameters

Figures 5 and 6 show the pressure dependence of the phonon frequencies of $NdCrO_4$ and $DyCrO_4$, respectively. The solid lines represent the linear least-squares fits for different Raman modes. The fitted results give the slopes of phonon frequency versus pressure $\partial\omega_i/\partial p$, as well as the zero-pressure phonon frequencies ω_{0i}, where the subscript i

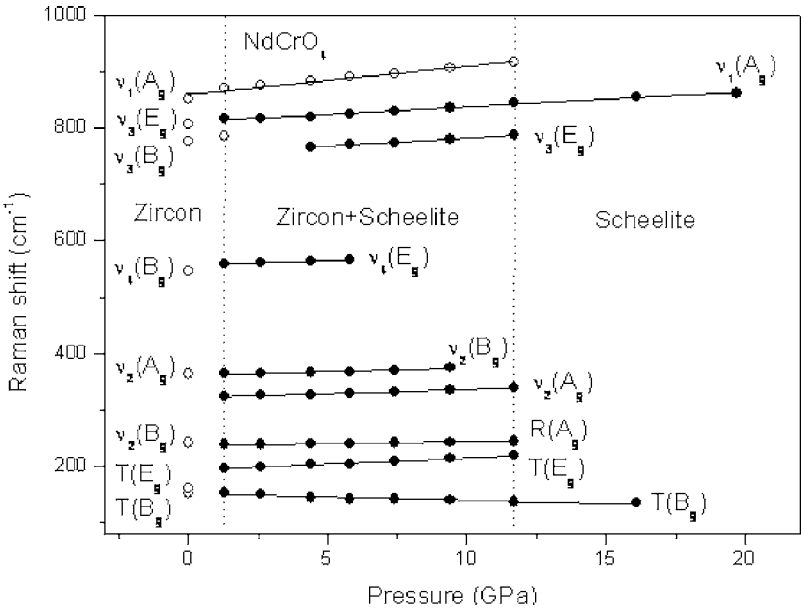

FIG. 5. Pressure dependence of the phonon frequencies of $NdCrO_4$ in 0–19.7 GPa. The open and solid circles represent the zircon and scheelite phases, respectively. The vertical dot lines show different phase regions. The solid lines are linear least-squares fits, giving the slope of $\partial\omega_i/\partial p$.

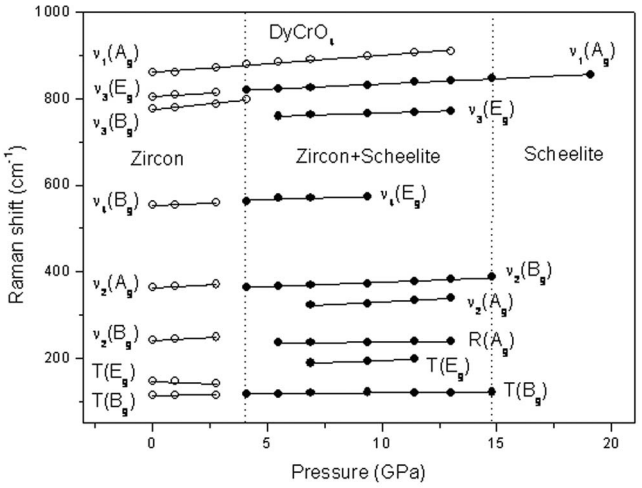

FIG. 6. Pressure dependence of the phonon frequencies of $DyCrO_4$ in 0–19.1 GPa. The open and solid circles represent the zircon and scheelite phases, respectively. The vertical dot lines show different phase regions. The solid lines are linear least-squares fits, giving the slope of $\partial\omega_i/\partial p$.

denotes the *i*th Raman mode, as listed in Table II. Obviously, the stretching modes exhibit the larger shift speed with pressure than other modes. In addition, a soft mode with a negative pressure coefficient is observed at the scheelite-type $NdCrO_4$. It implies that a second structural phase transition (most likely from scheelite to fergusonite phase[37,38]) will probably happen at a higher pressure than that reached in our experiments.[34]

The mode Grüneisen parameters γ_i can be calculated according to the formula $\gamma_i=-(\partial \ln \omega_i/\partial \ln V)=B_0/\omega_{0i}\partial\omega_i/\partial p$, where V and B_0 are the unit cell volume and bulk modulus, respectively. For the zircon- and scheelite-type ABO_4 compounds, a useful experiential formula, $B_0(\mathrm{GPa})=(610\pm110)Z_A/d_{A\text{-}O}^3$, was proposed by Errandonea *et al.* to calculate the bulk modulus,[37] where Z_A and $d_{A\text{-}O}$ are the formal charge for an *A*-site cation and the average *A*-*O* distance (in angstroms) in AO_8 units, respectively. According to this formula, the bulk modulus was calculated to be 135 and 137 GPa for the zircon- and scheelite-type $DyCrO_4$, respectively. Consequently, the mode Grüneisen parameters were obtained, as shown in Table II.

TABLE II. Ambient-pressure phonon frequencies ω_{0i}, pressure derivatives of frequencies $\partial\omega_i/\partial p$, and mode Grüneisen parameters γ_i for various Raman modes of $RCrO_4$.

Raman mode	ω_{0i} (cm^{-1})	$\partial\omega_i/\partial p$ (cm^{-1} GPa^{-1})	γ_i
	Zircon-type $DyCrO_4$		
$T(B_g)$	114	0.45	0.53
$T(E_g)$	150	−2.14	−1.93
$\nu_2(B_g)$	241	2.85	1.60
$\nu_2(A_g)$	363	2.88	1.07
$\nu_4(B_g)$	553	2.16	0.53
$\nu_3(B_g)$	777	5.48	0.95
$\nu_3(E_g)$	805	3.39	0.57
$\nu_1(A_g)$	860	3.97	0.62
	Scheelite-type Dy/$NdCrO_4$		
$T(B_g)$	117/151	0.33/−1.16	0.39/−0.92
$T(E_g)$	175/194	1.98/2.09	1.55/1.29
$R(A_g)$	232/237	0.54/0.55	0.32/0.28
$\nu_2(A_g)$	303/322	2.79/1.40	1.26/0.52
$\nu_2(B_g)$	356/362	2.01/1.24	0.77/0.41
$\nu_4(B_g)$	~417/430	⋯	⋯
$\nu_4(E_g)$	559/557	1.48/1.61	0.36/0.34
$\nu_3(E_g)$	750/753	1.65/2.92	0.30/0.47
$\nu_1(A_g)$	810/812	2.44/2.67	0.41/0.39

Concerning $NdCrO_4$, the average Nd–O distance of the zircon phase was determined to be 2.477 Å,[9] but no crystallographic data are available for the scheelite phase at present. Experiments show that the change of the average *A*-*O* distance is very small in the zircon-scheelite transition.[12,29] For example, $d_{A\text{-}O}$ is 2.362(3) and 2.366(4) Å in the zircon- and scheelite-type $YCrO_4$, respectively.[29] Therefore, we used here the zircon-phase average Nd–O bond length to calculate the bulk modulus of the scheelite-type $NdCrO_4$. It was determined to be 120 GPa, and the mode Grüneisen parameters for this phase were then obtained, as presented in Table II. Unfortunately, the data we collected for the zircon-type $NdCrO_4$ are not enough to calculate its mode Grüneisen parameters in the present paper.

IV. CONCLUSION

The high-pressure structural properties have been studied on the zircon-type $RCrO_4$ compounds by using Raman scattering methods at room temperature. The crystal structure of $NdCrO_4$ is very sensitive to pressure. A structural phase transition occurs at the onset of 1.3 GPa. A similar structural conversion is observed in $DyCrO_4$, but the transition pressure increases to 4.1 GPa. Pressure-induced structural transitions are sluggish in these two compounds at room temperature. The zircon phase and the new phase coexist in 1.3–11.7 and 4.1–13.0 GPa in $NdCrO_4$ and $DyCrO_4$, respectively. Pressure-released Raman spectra show that the high-pressure new phases that appeared in both of them can be quenched to ambient conditions. A scheelite-type $DyCrO_4$ bulk sample was prepared at 6 GPa and 450 °C. Moreover, it exhibits the same Raman vibrations as that of the pressure-released $DyCrO_4$. This fact convincingly confirms the zircon-to-scheelite structural phase transitions of $RCrO_4$ at the high pressure that we used. Finally, we calculated the mode Grüneisen parameters of $RCrO_4$ by using the formula $\gamma_i=B_0/\omega_{0i}\partial\omega_i/\partial p$. The bulk moduli of both the zircon- and scheelite-type phases were determined according to Errandonea's method.

ACKNOWLEDGMENTS

This work was partly supported by the National Natural Science Foundation and the Ministry of Science and Technology of China through the research projects (Grant Nos.2005CB724402, 2007CB925003, and 10674160).

[1] J. M. Hanchar and P. W. O. Hoskin, *Zircon*, Reviews in Mineralogy Vol. 53 (Mineralogical Society of America, Washington, D. C., 2003).
[2] G. Weber and K. J. Range, Z. Naturforsch. **51b**, 751 (1996).
[3] J. A. Baglio and G. Gashurov, Acta Crystallogr., Sect. B: Struct. Crystallogr. Cryst. Chem. **24**, 292 (1968).
[4] D. J. Salt and G. Hornung, J. Am. Ceram. Soc. **50**, 549 (1967).

[5]K. J. Range, M. Wildenauer, and M. Andratschke, Z. Kristallogr. **211**, 815 (1996).
[6]G. Buisson, F. Tcheou, F. Sayetat, and K. Scheunemann, Solid State Commun. **18**, 871 (1976).
[7]M. Steiner, H. Dachs, and H. Ott, Solid State Commun. **29**, 231 (1979).
[8]R. T. Harley, W. Hayes, and S. R. P. Smith, Solid State Commun. **9**, 515 (1971).
[9]K. Tezuka and Y. Hinatsu, J. Solid State Chem. **160**, 362 (2001).
[10]A. Jayaraman, G. A. Kourouklis, G. P. Espinosa, A. S. Cooper, and L. G. Van Uitert, J. Phys. Chem. Solids **48**, 755 (1987).
[11]S. J. Duclos, A. Jayaraman, G. A. Kourouklis, A. S. Cooper, and R. G. Maines, J. Phys. Chem. Solids **50**, 769 (1989).
[12]X. Wang, I. Loa, K. Syassen, M. Hanfland, and B. Ferrand, Phys. Rev. B **70**, 064109 (2004).
[13]A. Reid and A. E. Ringwood, Earth Planet. Sci. Lett. **6**, 205 (1969).
[14]L. G. Liu, Earth Planet. Sci. Lett. **44**, 390 (1979).
[15]K. Kusaba, T. Yagi, M. Kikuchi, and Y. Syono, J. Phys. Chem. Solids **47**, 675 (1986).
[16]E. Knittle and Q. Williams, Am. Mineral. **78**, 245 (1993).
[17]W. V. Westrenen, M. R. Frank, J. M. Hanchar, Y. Fei, R. J. Finch, and C. S. Zha, Am. Mineral. **89**, 197 (2004).
[18]Y. W. Long, W. W. Zhang, L. X. Yang, Y. Yu, R. C. Yu, S. Ding, Y. L. Liu, and C. Q. Jin, Appl. Phys. Lett. **87**, 181901 (2005).
[19]Y. W. Long, L. X. Yang, S. J. You, Y. Yu, R. C. Yu, C. Q. Jin, and J. Liu, J. Phys.: Condens. Matter **18**, 2421 (2006).
[20]H. Schwarz, Z. Anorg. Allg. Chem. **322**, 1 (1963).
[21]E. Jimenez, J. Isasi, and R. Saez-Puche, J. Alloys Compd. **312**, 53 (2000).
[22]R. Saez-Puche, E. Jimenez, J. Isasi, M. T. Fernandez-Diaz, and J. L. Garcia-Munoz, J. Solid State Chem. **171**, 161 (2003).
[23]K. Tezuka, Y. Doi, and Y. Hinatsu, J. Mater. Chem. **12**, 1189 (2002).
[24]E. Jimenez, J. Isasi, and R. Saez-Puche, J. Solid State Chem. **164**, 313 (2002).
[25]E. Jimenez, J. Isasi, M. T. Fernandez, and R. Saez-Puche, J. Alloys Compd. **344**, 369 (2002).
[26]E. Jimenez, P. Bonville, J. A. Hodges, P. C. M. Gubbens, J. Isasi, and R. Saez-Puche, J. Magn. Magn. Mater. **272**, 571 (2004).
[27]E. Jimenez-Melero, N. H. Van Dijk, W. H. Kraan, P. C. M. Gubbens, J. Isasi, and R. Saez-Puche, J. Magn. Magn. Mater. **288**, 1 (2005).
[28]Y. W. Long, L. X. Yang, Y. Yu, F. Y. Li, R. C. Yu, S. Ding, Y. L. Liu, and C. Q. Jin, Phys. Rev. B **74**, 054110 (2006).
[29]Y. W. Long, L. X. Yang, Y. Yu, F. Y. Li, R. C. Yu, and C. Q. Jin, Phys. Rev. B **75**, 104402 (2007).
[30]H. K. Mao, J. Xu, and P. M. Bell, J. Geophys. Res. **91**, 4673 (1986).
[31]S. A. Miller, H. H. Caspers, and H. E. Rast, Phys. Rev. **168**, 964 (1968).
[32]E. Sarantopoulou, Y. S. Raptis, E. Zouboulis, and C. Raptis, Phys. Rev. B **59**, 4154 (1999).
[33]A. Muller, E. J. Baran, and R. O. Carer, Struct. Bonding (Berlin) **26**, 81 (1976).
[34]F. J. Manjon, D. Errandonea, N. Garro, J. Pellicer-Porres, P. Rodriguez-Hernández, S. Radescu, J. Lopez-Solano, A. Mujica, and A. Munoz, Phys. Rev. B **74**, 144112 (2006).
[35]D. Errandonea, Y. Meng, M. Somayazulu, and D. Hausermann, Physica B **355**, 116 (2005).
[36]V. S. Stubican and R. Roy, J. Appl. Phys. **34**, 1888 (1963).
[37]D. Errandonea, J. Pellicer-Porres, F. J. Manjon, A. Segura, Ch. Ferrer-Roca, R. S. Kumar, O. Tschauner, P. Rodriguez-Hernández, J. Lopez-Solano, S. Radescu, A. Mujica, A. Munoz, and G. Aquilanti, Phys. Rev. B **72**, 174106 (2005).
[38]D. Errandonea, J. Pellicer-Porres, F. J. Manjon, A. Segura, Ch. Ferrer-Roca, R. S. Kumar, O. Tschauner, J. Lopez-Solano, P. Rodriguez-Hernández, S. Radescu, A. Mujica, A. Munoz, and G. Aquilanti, Phys. Rev. B **73**, 224103 (2006).